

Notes

respectively as $(\Delta G^{\circ}_T)_{el}$ and $(E^{\circ}_T)_{el}$. The free energy change in (10) can be written as

$$(\Delta G^{\circ}_T)_{pr} = RT \ln K \quad (12)$$

where K is the dissociation constant of the acid $H_m\text{Red}$ (K is the inverse of the equilibrium constant of eq 10). The equation of free-energy balance

$$\Delta G^{\circ}_T = (\Delta G^{\circ}_T)_{el} + (\Delta G^{\circ}_T)_{pr} \quad (13)$$

can be combined with eq 11 and 12 to yield (at 298 K)

$$E^{\circ}_{298} = (E^{\circ}_{298})_{el} + (0.059/n)pK \quad (14)$$

In the specific cases of equilibria 6 and 7, pK of eq 14 can be expressed respectively as (see eq 1 and 2) $pK_1 + pK_2$ and pK_2 . The values of E°_{298} calculated from eq 14 using experimental values of $(E^{\circ}_{298})_{el}$ and pK for Fe(III)-Fe(II) systems and the corresponding Ni(III)-Ni(II) systems^{4,6} are set out in Table III. The last entry in Table III refers to the Ni(IV)-Ni(II) couple^{4,6}



The electron-transfer couple $\text{Ni}(\text{Me}_2\text{L})^{2+} + 2e^- \rightleftharpoons \text{Ni}(\text{Me}_2\text{L})$ is not known experimentally. However, the two one-electron couples $\text{Ni}(\text{Me}_2\text{L})^{2+} + e^- \rightleftharpoons \text{Ni}(\text{Me}_2\text{L})^+$ and $\text{Ni}(\text{Me}_2\text{L})^+ + e^- \rightleftharpoons \text{Ni}(\text{Me}_2\text{L})$ are well characterized.^{4,6} From consideration of free energy balance it is readily shown that

$$E^{\circ}_{298} = 1/2 [(E^{\circ}_{298})_{el1} + (E^{\circ}_{298})_{el2} + 0.059(pK_1 + pK_2)] \quad (16)$$

where E°_{298} is the redox potential of couple (15), $(E^{\circ}_{298})_{el1}$ and $(E^{\circ}_{298})_{el2}$ are the redox potentials of the one-electron couples, and pK_1 and pK_2 refer to the first and second dissociation of $\text{Ni}(\text{H}_2\text{Me}_2\text{L})^{2+}$.

The agreement between calculated and experimental formal electrode potentials is excellent in all cases (Table III). The separation of the total free energy of reactions of type (3) into electron-transfer and proton-transfer contributions is valid.

Registry No. Fe(H₂EtMeL)(ClO₄)₂, 62107-58-8; Fe-(H₂MeEtL)(ClO₄)₂, 62078-93-7; Fe(H₂Me₂L)(ClO₄)₂, 55758-57-1; Fe(HMe₂L)⁺, 60306-12-9; Fe(Me₂L)⁺, 60196-59-0; Fe(Me₂L), 60306-13-0; Fe(EtMeL)⁺, 62078-91-5; Fe(EtMeL), 62078-90-4; Fe(MeEtL)⁺, 62078-89-1; Ni(Me₂L)⁺, 59980-38-0; Ni(HMe₂L)⁺, 60306-03-8; Ni(H₂Me₂L)²⁺, 55188-31-3; Ni(Me₂L)²⁺, 55188-33-5; triethylenetetramine, 112-24-3; isonitrosoethyl ethyl ketone, 32818-79-4.

References and Notes

- (1) E. I. Steifel, *Proc. Natl. Acad. Sci. U.S.A.*, **70**, 988 (1973).
- (2) J. G. Mohanty, R. P. Singh, and A. Chakravorty, *Inorg. Chem.*, **14**, 2178 (1975).
- (3) J. G. Mohanty and A. Chakravorty, *Indian J. Chem., Sect. A*, **14**, 200 (1976).
- (4) J. G. Mohanty and A. Chakravorty, *Inorg. Chem.*, **15**, 2912 (1976).
- (5) R. S. Nicholson and I. Shain, *Anal. Chem.*, **36**, 706 (1964).
- (6) J. G. Mohanty and A. Chakravorty, *Inorg. Chim. Acta*, **18**, L33 (1976).

Contribution from the Department of Chemistry and Materials Research Center, Northwestern University, Evanston, Illinois, 60201

Single-Crystal Electron Nuclear Double Resonance Studies of Silver(II) and Copper(II) Tetraphenylporphyrins

Theodore G. Brown, Jeffrey L. Petersen, George P. Lozos, James R. Anderson, and Brian M. Hoffman*

Received October 16, 1976

AIC607581

The importance of understanding the bonding in metal-porphyrins has led us to undertake a comparative study of

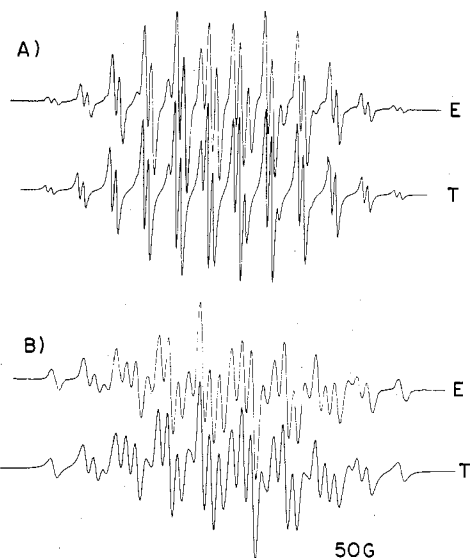


Figure 1. Experimental EPR spectra of AgTPP in (H₂O)ZnTPP (E) and computer simulations (T) employing the spin-Hamiltonian parameters of Table I: (A) H parallel to g_1 ; (B) H along Ag-N axis. Unresolved proton and/or silver isotope interactions were allowed for by using Gaussian line widths of 4 and 6 G, respectively, in simulating (A) and (B).

silver(II) and copper(II) tetraphenylporphyrins (TPP) through the use of electron nuclear double resonance (ENDOR) on oriented, dilute single crystals.¹ The enhanced resolution available from ENDOR² uniquely permits one to map out the odd-electron distribution within these molecules and to compare the M-N bonding in the two systems, and gives information about their geometric configurations as well.

Experimental Section

Metalloporphyrins were prepared by published procedures.³ AgTPP and ⁶³CuTPP, were separately doped into single crystals of (H₂O)ZnTPP by slow evaporation from toluene solution, 1 mol % in dopant. EPR and ENDOR spectra were obtained as described elsewhere.^{4,5} The lowest available temperature, 20 K, gave optimal ENDOR for CuTPP, but AgTPP afforded the best ENDOR at 30 K.

(H₂O)ZnTPP crystals exhibit a single molecule per unit cell, with C_4 , but $\sim C_{4v}$, symmetry. There is a twofold disorder in which the H₂O can point "up" or "down"; the statistically averaged molecule lies in a mirror plane and exhibits C_{4h} symmetry.⁶ This disorder does not affect the EPR or ENDOR spectra, and only one site is observed spectroscopically. Since the g tensors for both dopants are axial,¹ the magnetic field, H , was aligned along g_1 or along g_2 , lying in the molecular mirror plane ($\pm 1^\circ$), by employing the orientation dependence of the EPR signal. Orientation of the field within the molecular plane was obtained from the ENDOR measurements (vide infra).

Results

The angular-dependent EPR spectra of AgTPP and ⁶³CuTPP in (H₂O)ZnTPP give g values in agreement with those reported by Manoharan and Rogers (MR) for an H₂TPP host.¹ The spectra in the (H₂O)ZnTPP host are generally better resolved, in part due to the lower temperatures employed and, for copper, because of our use of isotopically pure ⁶³Cu. In a general orientation the spectra exhibit hyperfine splitting (hfs) from the central metal ion, in some cases with distinguishable patterns arising from ¹⁰⁷Ag and ¹⁰⁹Ag, and from pairs of equivalent pyrrole nitrogens (Figure 1). The metal coupling constants were obtained from EPR; because of considerable overlapping of lines, no effort was made to directly analyze the ¹⁴N pattern (but vide infra).

No evidence of proton hfs is discernible in the EPR (Figure 1); both AgTPP and CuTPP, however, show well-resolved

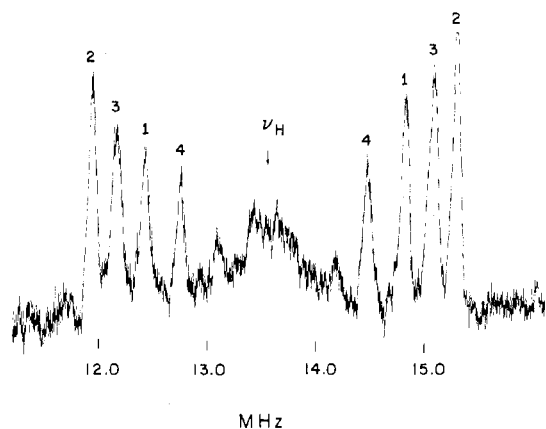


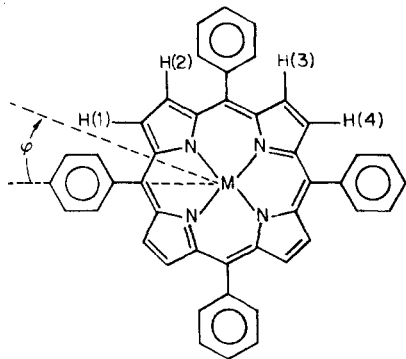
Figure 2. Proton ENDOR spectrum of AgTPP with H lying in the molecular plane, $\varphi = 75^\circ$ (see text), showing well-resolved doublets from the four distinct proton pairs and the poorly resolved phenyl-ring resonances ($T = 30$ K, $\nu_{\text{microwave}} = 9124$ MHz).

ENDOR from the pyrrole protons (Figure 2), as well as smaller splittings from phenyl protons. The ENDOR spectrum of n equivalent protons is one pair of lines, split approximately symmetrically about the NMR frequency of the free proton (ν_H), provided that $\nu_H \gg A_i^H$; the actual formula for the two observed ENDOR frequencies in this limit⁷ is

$$\nu_{\pm} = K_{\pm} = \left[\sum_{i=1}^3 l_i^2 \left(\pm \frac{g_i A_i^H}{2g} - g^H \beta_n H \right)^2 \right]^{1/2} \quad (1)$$

where l_i is the direction cosine between H and the i th hfs tensor axis, g_i and A_i^H are the i th principal values of the g and hfs tensors, g^H and β_n are the proton g -factor nuclear magneton, respectively, and $g^2 = \sum_{i=1}^3 l_i^2 g_i^2$.

When the external field lies at a general direction in the porphyrin plane, the proton ENDOR of AgTPP shows four intense doublets from the pyrrole protons as well as lines from phenyl protons. Observation of just four pyrrole doublets indicates the equivalence of the proton in pairs, labeled 1–4, related by reflection through the metal, as required by the crystal environment.



ENDOR spectra of the pyrrole protons were collected as a function of angle and the data for each pair were fit to eq 1. The maximum splitting A_i^H lies in the molecular plane and the angle between the $M-C_m$ vector and the direction of this splitting, φ_0 , was an additional fitting parameter. With the magnetic field normal to the molecular plane, two overlapping and barely resolved doublets corresponding to the pyrrole protons were observed. The results for the proton ENDOR of $^{63}\text{CuTPP}$ were analogous, with the exception that only a single pair of lines was evident in the spectrum with the field along g_{\parallel} . The resulting hyperfine parameters for both systems are presented in Table I.

Well-resolved ^{14}N ENDOR was also seen. For n equivalent, noninteracting ^{14}N nuclei, four ENDOR lines are expected.²

Table I. Nuclear Hyperfine Parameters (MHz) for MTPP in the $(\text{H}_2\text{O})\text{ZnTPP}$ Host^{a,b}

M	Atom	A_1	A_2	A_3	$\varphi_0,^c$ deg	
Ag	^{107}Ag	174 ^d	88.376	88.376		
	^{109}Ag	187 ^d	102.001	102.001		
	^{14}N	79.028	60.980	62.906		
	Protons ^e					
	H(1)	3.566	1.729	1.145	24.7	
	H(2)	3.443	1.618	1.232	65.1	
	H(3)	3.578	1.749	1.145	114.6	
	H(4)	3.462	1.648	1.232	155.4	
Cu	^{63}Cu	615 ^d	102.674	102.674		
	^{14}N	54.474	44.264	44.065		
	Protons ^f					
		H(1)	2.52	0.74	0.80	27.5
		H(2)	2.45	0.71	0.80	64.0
		H(3)	2.41	0.66	0.80	117.2
	H(4)	2.49	0.69	0.80	154.3	

^a Unless noted, values are obtained by ENDOR as discussed in the text, with an estimated precision for M and ^{14}N parameters of ± 0.005 MHz; the accuracy of ^{14}N values may be somewhat less, as described in the text, but is estimated to be better than ± 0.02 MHz. Estimated errors for proton parameters are noted. It can be shown that all quantities are positive. ^b Tensor orientations and the definition of φ_0 are given in the text. Note, however, that A_1^M is obtained when H is along g_{\parallel} , but A_1^N is obtained when H is along the M–N bond. ^c ± 1.0 deg. ^d Obtained from EPR spectra; ± 3 MHz. ^e ± 0.015 MHz. ^f ± 0.05 MHz.

When $A_i^N \gg \nu_N$, as is presently the case, the frequencies to first order⁷ are

$$\nu_{\text{ENDOR}} = (K/2) \pm \nu_N \pm P \quad (2)$$

where P is the angle-dependent quadrupole coupling and $K^2 g^2 = \sum_i l_i^2 g_i^2 (A_i^N)^2$.

For a perfect square of equivalent nitrogens around the central metal, an arbitrary orientation of the external field would leave the inversion-related pairs equivalent, and two four-line patterns would be expected. Two patterns are in fact observed, which merge at $\varphi = 0^\circ$ when H is in the molecular plane and when H is normal to the molecular plane, as would be expected by symmetry if all nitrogens are equivalent. However, the individual patterns exhibit more than four lines. This is not due to a chemical inequivalence within the pairs but rather arises from the large electronic–nuclear interaction which produces an effective coupling between the equivalent nuclei.⁸ In the presence of this feature, the detailed analysis required to obtain the exact quadrupole and hyperfine coupling constants is quite complicated⁹ and will be presented later. The principal values of an ^{14}N hfs tensor can, however, be extracted from the spectra to good accuracy by applying second-order corrections to the average of the frequencies of the lines in the pattern from an equivalent ^{14}N pair.¹⁰ These corrections are relatively small (< 0.02 MHz). With H in plane, along $\varphi = 45^\circ$, we obtain both A_1^N and A_2^N , the values with H along and perpendicular to an M–N bond; A_3^N is observed when H is normal to the plane. The ^{14}N hyperfine tensors for AgTPP and CuTPP are also presented in Table I.

The largest tensor value, A_1^M , is observed when H is along g_{\parallel} and was obtained only by EPR. ENDOR from ^{107}Ag , ^{109}Ag , and ^{63}Cu was observed for H in the molecular plane; for both metals the tensor is axial, $A_2^M = A_3^M$.

Discussion

Both metalloporphyrins exhibit finite values of $a^H = (\sum_{i=1}^3 A_i^H)/3$, indicating σ delocalization of the “metal ion odd electron” through four bonds onto the protons. For AgTPP, not all proton pairs have the same a^H , with protons 1 and 3 having one value and protons 2 and 4 a different value. Indeed, the observation of two doublets for H along g_{\parallel} directly shows the existence of two classes of protons. This indicates

that within the limits of resolution, a guest AgTPP can have either S_4 or the actual site symmetry C_4 but does not possess the approximate C_{4v} symmetry or higher. On the other hand, within a slightly larger error, the isotropic hfs for all four pyrrole proton pairs of CuTPP are equal and only one doublet is observed when H is along $g_{||}$. Thus, there is no evidence of symmetry lower than C_{4v} for CuTPP.

For both AgTPP and CuTPP the proton hfs tensors are anisotropic and, furthermore, the observed dipolar contributions are greater for Ag than for Cu and greater than would be calculated from the classical point-dipolar formula. In addition, for the two protons on a given pyrrole ring, the vectors at angles of φ_0 make a greater angle with the vector along the M-N bond than would be calculated from the crystallographically determined M-H vectors.¹¹ These features all arise from the distributed nature of the unpaired-electron cloud. They show that the odd electron cannot be considered as a point-dipole located at the metal ion position, and that the extent of the odd-electron delocalization is greater for silver than for copper.

The ^{14}N hfs tensor is essentially axial with the unique direction along the M-N bond; the slight deviations from axial symmetry again appear to be attributable to the extended nature of the d orbital.¹² These tensor components obtained by ENDOR can be successfully used in computer simulations of the observed EPR spectra (Figure 1). Features of the EPR spectra in an H_2TPP host which were previously suggested to indicate nitrogen nonplanarity¹ now appear to arise from a partial resolution of the unequal coupling constants for the two pairs of inversion-related nitrogens.

The ^{14}N hfs parameters further give information about the relative covalency of the Ag-N bond, involving bonding with a 4d orbital, as opposed to the Cu-N bond. The ^{14}N isotropic coupling constant, $a^N = (\sum_i A^N_i)/3$, is proportional to the nitrogen s-orbital population of the odd electron. As a simplified illustration, if a fixed (sp^2) hybridization at N is assumed and polarization effects are ignored, then the ratio $a^N(\text{Ag})/a^N(\text{Cu})$ gives the ratio of the contribution of nitrogen orbitals to the odd-electron wave function. Use of the data in Table I indicates that the contribution is roughly 40% greater in AgTPP and further shows that the d-orbital contribution to the odd-electron wave function for CuTPP is $\sim 65\%$, while that for AgTPP is only $\sim 50\%$.¹³ This change in covalency with metal atom is in interesting contrast with the rough constancy of nitrogen hyperfine splittings for a number of different copper porphyrins and phthalocyanine.¹⁴ Completion of the complex analysis of the ^{14}N ENDOR patterns will allow us to obtain the quadrupole coupling parameters, which measure the asymmetry of the total electron distribution around nitrogen; these results will be combined with those presented here in a detailed discussion of the electronic structure of these systems.

Acknowledgment. This work has been supported by the National Science Foundation through Grant DMR 7601057 to the Northwestern University Materials Research Center, by National Science Foundation Grant BMS 00478, and by National Institutes of Health Grant HL-13531. We thank Professor J. L. Hoard for the details of the structure of AgTPP.

Registry No. AgTPP, 14641-64-6; CuTPP, 14172-91-9; H_2OZnTPP , 16456-79-4.

References and Notes

- (1) For a single crystal EPR study of CuTPP and AgTPP, see P. T. Manoharan and M. T. Rogers, *Electron Spin Reson. Met. Complexes, Proc. Symp.*, 1968, 143 (1969).
- (2) L. Kevan and L. D. Kispert, "Electron Spin Double Resonance Spectroscopy", Wiley-Interscience, New York, N.Y., 1976.
- (3) A. D. Adler, F. R. Longo, F. Kampas, and J. Kim, *J. Inorg. Nucl. Chem.*, **32**, 927 (1969).
- (4) B. M. Hoffman, C. J. Weschler, and F. Basolo, *J. Am. Chem. Soc.*, **98**, 5473 (1976).
- (5) G. P. Lozos, Ph.D. Dissertation, Northwestern University, 1974.
- (6) M. D. Glick, G. H. Cohen, and J. L. Hoard, *J. Am. Chem. Soc.*, **89**, 1996 (1967).
- (7) A. Abragam and B. Bleaney, "Electron Paramagnetic Resonance of Transition Ions", Clarendon Press, Oxford, 1970.
- (8) V. Ya. Zevin, S. S. Ishchenko, and M. A. Ruban, *Zh. Eksp. Teor. Fiz.*, **55**, 2108 (1968).
- (9) After the submission of this paper, an extended discussion of the difficulties created by the nuclear-nuclear coupling has appeared: A. Schweiger, F. Graf, G. Rist, and Hs. H. Günthard, *Chem. Phys.*, **17**, 155 (1976).
- (10) Reference 7, Chapter 3.
- (11) For a discussion of the AgTPP and CuTPP structures, see J. L. Hoard, *Porphyrins Metalloporphyrins* (1975).
- (12) Note that the ^{14}N tensors of ref 1 are in error. Their reported A^N and B^N correspond to A^N_3 and to $(A^N_1 + A^N_2)/2$, respectively.
- (13) For the unit spin-density values, see J. R. Morton, J. R. Rowlands, and D. H. Whiffen, *Natl. Phys. Lab., (U. K.), Circ.*, No. BPR 1.3.
- (14) For a recent compilation, see P. W. Lau and W. C. Lin, *J. Inorg. Nucl. Chem.*, **37**, 2389 (1975).

Contribution from the Department of Chemistry,
Tulane University, New Orleans, Louisiana 70118

Spectroscopic Properties of Vanadium(II), Manganese(II), and Nickel(II) in Crystals of CsCdBr_3

Gary L. McPherson* and Kenneth O. Devaney

Received November 1, 1976

AIC60779V

A considerable number of double salts of the formula AMX_3 (where A is a univalent cation, M a divalent metal ion, and X a halide) have been isolated and characterized. When A is a large ion such as cesium or tetramethylammonium, a linear-chain structure similar to that of CsNiCl_3 or $(\text{C}_2\text{H}_5)_4\text{NMnCl}_3$ is usually observed. This structure can be described as a parallel array of infinite linear chains of $[\text{MX}_6]^{4-}$ octahedra-sharing faces. The large cations occupy positions between chains. The spectroscopic and magnetic properties of transition metal salts of this type have been of considerable interest because of the strong one-dimensional character of their structure.

The magnesium salts CsMgCl_3 , CsMgBr_3 , and CsMgI_3 have been shown to be isostructural with CsNiCl_3 .¹⁻³ These diamagnetic materials have proved to be useful host lattices in a variety of spectroscopic and magnetic investigations.^{1,2,4-11} Recently it has been found that the cadmium salt CsCdBr_3 adopts the CsNiCl_3 structure. Thus, CsCdBr_3 is also a suitable diamagnetic host material for studying the properties of "isolated" transition metal ions in a linear-chain AMX_3 lattice. This paper presents the results of EPR studies of single crystals of CsCdBr_3 doped with divalent vanadium, manganese, and nickel. The ligand field spectrum of divalent nickel in CsCdBr_3 crystals is also reported. The properties of the paramagnetic ions in CsCdBr_3 and CsMgBr_3 are carefully compared in order to determine how great an effect a change in host lattice has on an ion's behavior in this series of compounds.

Experimental Section

Preparation of Materials. The salt CsCdBr_3 was crystallized by slow evaporation of aqueous HBr solutions containing equimolar amounts of cesium bromide and cadmium acetate dihydrate. The white crystalline solid was dried at 120 °C and stored in stoppered vials. The material is not noticeably hygroscopic. Anal. Calcd for CsCdBr_3 : Br, 49.36. Found: Br, 49.03.

Crystal Growth. Single crystals suitable for spectroscopic and x-ray work were grown from the melt by the Bridgman method. Doped crystals for EPR study were prepared by adding $\sim 0.1\%$ (by weight) of the appropriate transition metal salt to the CsCdBr_3 . The crystal